

Article

Study of Morphology and Corrosion Behavior of Aluminum Coatings on Steel Substrates under Simulated Acid Rain Conditions

Bo Li ¹, Lei Fan ¹, Yi Wen ¹, Jinhang He ¹, Jianfeng Su ², Shiyuan Zhou ³, Shifeng Liu ^{3,*}  and Zhiqing Zhang ³¹ Electric Power Research Institute, Guizhou Power Grid Limited Liability Company, Guiyang 550000, China² Anshun Power Supply Bureau, Guizhou Power Grid Limited Liability Company, Anshun 561000, China³ College of Materials Science and Engineering, Chongqing University, Chongqing 400044, China

* Correspondence: liusf06@cqu.edu.cn

Abstract: In this paper, aluminum coatings were prepared on a steel substrate by thermal spraying, and the corrosion morphology and corrosion resistance of the coating were investigated by salt spray and immersion tests. The results showed that after three months of salt spray tests, the coating still exhibited a surface morphology without significant damage and had good damage tolerance. Further effective protection of the substrate can be achieved by spraying the coating surface with paint. After three months of immersion test, the corrosion rate of samples with thicker coatings was located between 0.002 mm/y and 0.005 mm/y, and only a small amount of corrosion products was observed on the coating surface. The coated samples after salt spray and immersion tests maintained sufficient adhesion (17.07 MPa and 19.25 MPa), and the surface aluminum coating was highly reliable for protection of the steel substrate. In general, the reliability of the coating can be further improved by painting the surface of the thicker Al coating. This provides more ideas for the protection of transmission and transformation equipment.

Keywords: aluminum coatings; salt spray; immersion; corrosion behavior



Citation: Li, B.; Fan, L.; Wen, Y.; He, J.; Su, J.; Zhou, S.; Liu, S.; Zhang, Z. Study of Morphology and Corrosion Behavior of Aluminum Coatings on Steel Substrates under Simulated Acid Rain Conditions. *Metals* **2023**, *13*, 613. <https://doi.org/10.3390/met13030613>

Academic Editor: Mosab Kaseem

Received: 15 February 2023

Revised: 6 March 2023

Accepted: 17 March 2023

Published: 19 March 2023



Copyright: © 2023 by the authors. Licensee MDPI, Basel, Switzerland. This article is an open access article distributed under the terms and conditions of the Creative Commons Attribution (CC BY) license (<https://creativecommons.org/licenses/by/4.0/>).

1. Introduction

With the development of industry, the acid content of the atmosphere is rapidly increasing [1–3]. Because of acid rain corrosion, metal facilities are at high risk of failure [4]. To protect these metal components and extend their service life, coatings are widely applied to material surfaces [5–7]. However, although the coatings have been successfully applied to a wide range of metal substrates, there are still many coating-related issues that need to be addressed, such as defects, smoothness, thickness, and cost [8].

As a common coating material for metal corrosion protection, aluminum (Al) metal surfaces can naturally form chemically stable and dense Al oxide film, and the repair ability of the oxide film is strong after being damaged, which can protect the metal against corrosion. Therefore, Al coatings are widely used in the protection of various metal substrates because of their reliable barrier protection effect [9–13]. In addition, it is evident from previous references that Al has a significant effect on the corrosion resistance and mechanical properties of the coating. After adding flaked Al to a polyamideimide–polytetrafluoroethylene bonded solid–lubricating composite coating, Li et al. [14] found that the aluminum could be uniformly dispersed in the coating, improving the denseness of the coating, while the corrosion resistance, hardness, and bonding of the coating were substantially improved. Feng et al. [15] found that the addition of moderate amounts of Al significantly improved the corrosion resistance of nickel-based coatings because of the formation of Al₂O₃ films. The addition of Al aggravated the lattice distortion and improved the solid solution strengthening effect, thus improving the hardness and wear resistance of the coatings. It can be

seen that Al is an excellent element for coating addition. Therefore, it is necessary and promising for the research of Al coatings.

Since steel is a common material used on power transmission and transformation equipment and it is exposed to highly corrosive environments for a long time, this can aggravate the corrosion of the steel substrate. Therefore, researchers have carried out a lot of exploration to prepare different states of Al coatings on steel substrates to study the protective effect of the coatings on the substrate [8,16–19].

Lee et al. [8] found that the addition of $\text{Ca}(\text{NO}_3)_2$ and $\text{NH}_4\text{H}_2\text{PO}_4$ to Al coatings of plain carbon steel resulted in denser coatings with crystalline forms, and then the corrosion resistance was improved. Li et al. studied the corrosion resistance of an Al coating on S355 steel in NaCl solution, and found that the Al coating had an obvious passivation tendency because of the protective barrier to the formation of oxide film on the Al coating. By isolating the chlorine corrosion and cathodic protection of sacrificial anode, the self-corrosion potential of Al coating is lower than that of substrate, which reduces the corrosion rate of steel substrate [16]. Ge et al. studied the formation and properties of superhydrophobic aluminum coating on a steel surface and found that the corrosion current density of this superhydrophobic aluminum coating was $1.36 \times 10^{-8} \text{ A cm}^{-2}$, significantly less than the corrosion rate ($1.18 \times 10^{-6} \text{ A cm}^{-2}$) of coating samples without superhydrophobic treatment in the same corrosive medium. This shows that the superhydrophobic treatment on the surface of Al coating can significantly improve the corrosion resistance of the material in seawater [17]. Ze et al. studied the effect of laser remelting on the microstructure and properties of Al coating on S355 steel. The results showed that the untreated Al coating was mainly composed of an Al phase, while the treated coating was composed of Al-Fe and AlO_4FeO_6 phases, and laser remelting could eliminate the pores and cracks in the coating. Compared with the untreated sample, the treated coating mainly exhibited uniform corrosion and pitting corrosion after the immersion test, and had better corrosion resistance [16]. Ashraf considered that annealing can change the morphology and corrosion resistance of Al coatings on low-carbon steel. The coatings annealed at 700°C had reduced grain size and showed the lowest corrosion current density ($1.504 \mu\text{A}/\text{cm}^2$), inert corrosion potential (-0.59 V versus Ag/AgCl), and higher charge transfer resistance ($511.76 \text{ k}\Omega\text{cm}^2$) [18]. It can be seen that researchers have carried out a lot of research on Al coatings on steel substrate, especially with regard to corrosion resistance.

However, in previous studies, corrosion resistance tests have been performed with short periods and lack results of continuous monitoring over long periods of time, which may not reflect the actual conditions of Al coatings in highly corrosive environments. In addition, studies on the effects of damage tolerance, coating thickness, and paint treatment on Al coatings have not been found. Therefore, more comprehensive studies are still needed to improve the understanding of Al coatings and to improve theoretical guidance for practical applications.

Thermal spraying is a common coating preparation method which can be divided into flame spraying [20], arc spraying [8], plasma spraying [21], and so on. At present, the microstructure of coatings prepared by flame spraying is not uniform and the porosity is high, and the equipment cost of plasma spraying is high and the working gas purity requirement is also very high. Therefore, in this paper, arc spraying, a very common and stable spraying method, was used for the preparation of coatings.

In this paper, carbon steel was selected as the substrate and two thicknesses (0.15 and 0.30 mm) of Al coatings were deposited on its surface by thermal spraying, and the damage and paint treatments were set up as control group experiments, respectively. Then, a salt spray test and immersion test were conducted to study the morphological changes, corrosion resistance, and adhesion properties of the coatings in the corrosive environment.

2. Materials and Methods

The substrate was S355 steel (two different sizes: $150 \text{ mm} \times 100 \text{ mm} \times 5 \text{ mm}$ for salt spray and $50 \text{ mm} \times 50 \text{ mm} \times 5 \text{ mm}$ for immersion tests), and the steel plate surface was

sandblasted with cold iron before spraying to achieve a relatively flat surface condition. Figure 1 shows the pseudo-color image of the surface roughness of the steel substrate after sandblasting. After sandblasting, the surface roughness of the substrate material was 56 μm , which satisfied the requirement that the surface roughness must be between 50 and 100 μm before spraying.

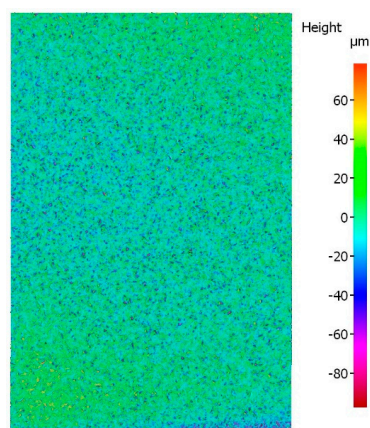


Figure 1. Pseudo-color image of S355 steel substrate after cold iron sandblasting.

Subsequently, the thermal spraying test was carried out on the steel substrate through the metallized Arc140 system. The diameter of commercial high-purity aluminum wire was 2.3 mm, and the spraying voltage, current, and air pressure were 30 V, 200 A, and 0.55 MPa, respectively. Finally, coating samples with thicknesses of about 0.15 mm and 0.30 mm were obtained. A set of samples was sealed with Sigmafast 278 primer (~0.25 mm dry film thickness (DFT) and Sigmadur 520 topcoat (~0.075 mm DFT) to explore the effect of painting on the coating. Moreover, some samples were scribed (50 × 2 mm) to test the damage tolerance of the coating. Prior to environmental testing, uncoated surfaces (backs, sides, and edges) were covered with a polymer resin (Belzona 4311) to ensure that the test surfaces were all coated.

Salt spray tests were performed in a mixture of 0.05 wt% NaCl and 0.35 wt% $(\text{NH}_4)_2\text{SO}_4$ solutions, and the samples were placed in a salt spray chamber and exposed to alternate wet cycles consisting of 1 h spraying and 1 h without spraying at 40 °C. The test was carried out for 3 months. Periodic inspection of specimens that have undergone salt spray testing and photography during the test. To minimize disruption, the photographs of the salt spray specimens were taken inside the chamber during the period without spraying. At each inspection, all corrosion-related features were photographed to keep a record. The samples for the immersion test were completely and stably submerged in 0.5 wt% NaCl and 3.5 wt% $(\text{NH}_4)_2\text{SO}_4$ solutions. The ambient temperature was also 40 °C. To perform electrochemical measurements, electrical connections were made on the specimens before test. The sample to be tested was made into a working electrode, Pt wire was used as a counter electrode, and Ag/AgCl was used as a reference electrode. The open-circuit potential (OCP) of the sample was measured with respect to the reference electrode using an ACM potentiostat. Electrochemical monitoring of the test coupons was undertaken throughout the testing, with OCP data being regularly recorded during 3 months. The corrosion rate can be obtained by the following calculation [22]:

$$CR = \frac{I_{corr}}{\rho} \times EW \times K_1 \quad (1)$$

where ρ is the density of Al, which is 2.71 g/cm^3 . EW is equivalent weight, and it is 8.99 for Al. K_1 is $3.27 \times 10^{-3} \text{ mm g}/\mu\text{A cm y}$. I_{corr} is the corrosion current, which can be obtained by the following formula:

$$I_{corr} = \frac{b_a \times b_c}{2.303 \times (b_a + b_c)} \times \frac{1}{R_p} \quad (2)$$

Anode slope (b_a) and cathode slope (b_c) can be obtained through Tafel analysis. R_p is the polarization resistance, and it is the slope of polarization curve and current density at zero polarization. The method of corrosion rate is obtained from ASTM G59 [22]. It is worth noting that both environmental tests were performed at $40 \text{ }^\circ\text{C}$ for 3 months.

The macro morphology of samples before and after environmental testing was observed by a digital camera. The microscopic morphology was characterized in detail by a TESCAN MIRA 3 field emission scanning electron microscope (SEM) with a voltage of 10 kV and a working distance of 10 mm. In addition, the adhesion changes of a group of samples before and after environmental exposure were also tested by a PosiTest AT-A adhesion tester (in accordance with ASTM D4541) [23].

To facilitate the recording of samples, all samples are listed in Table 1 with specific processing details. The corresponding numbers of the samples are used directly in the descriptions that follow.

Table 1. Samples involved in the test and their corresponding details.

Samples	Thickness/mm		Scribe $50 \times 2 \text{ mm}$		Painting	
	0.15	0.30	Yes	No	Yes	No
Uncorroded samples	#1	✓		✓		✓
	#2	✓		✓	✓	
	#3	✓		✓		✓
	#4	✓		✓	✓	
	#5		✓		✓	✓
	#6		✓		✓	✓
	#7		✓	✓		✓
	#8		✓	✓		✓
Salt spray test	#9	✓		✓		✓
	#10	✓		✓	✓	
	#11	✓		✓		✓
	#12	✓		✓	✓	
	#13		✓		✓	✓
	#14		✓		✓	✓
	#15		✓	✓		✓
	#16		✓	✓		✓
Immersion test	#17	✓		✓		✓
	#18		✓		✓	✓

3. Results and Discussions

3.1. Salt Spray Test

3.1.1. Macro Morphology

Figure 2 shows the macro morphology of the sprayed samples before and three months after the salt spray test (#1–#16). Before the salt spray test, the sprayed samples showed good surface morphology with no obvious defects in the coating and paint. After the salt spray test, the samples were gradually corroded. The paint and coating samples without any defects showed excellent performance. However, the samples with scribed lines had a lot of corrosion products in the scribed area. Rust contaminated the specimen. However, for thicker coatings with scribed lines, damage appeared to be limited, at least by visual inspection (Figure 2(#15)). The thin coating with scribed lines (about 0.15 mm) showed significant damage in the scribed area (Figure 2(#11)). The paint samples with scribed lines

further weakened the corrosion damage compared with the coated samples with scribed lines (Figure 2(#12)). However, this effect was not evident in samples with thick coatings (Figure 2(#16)).

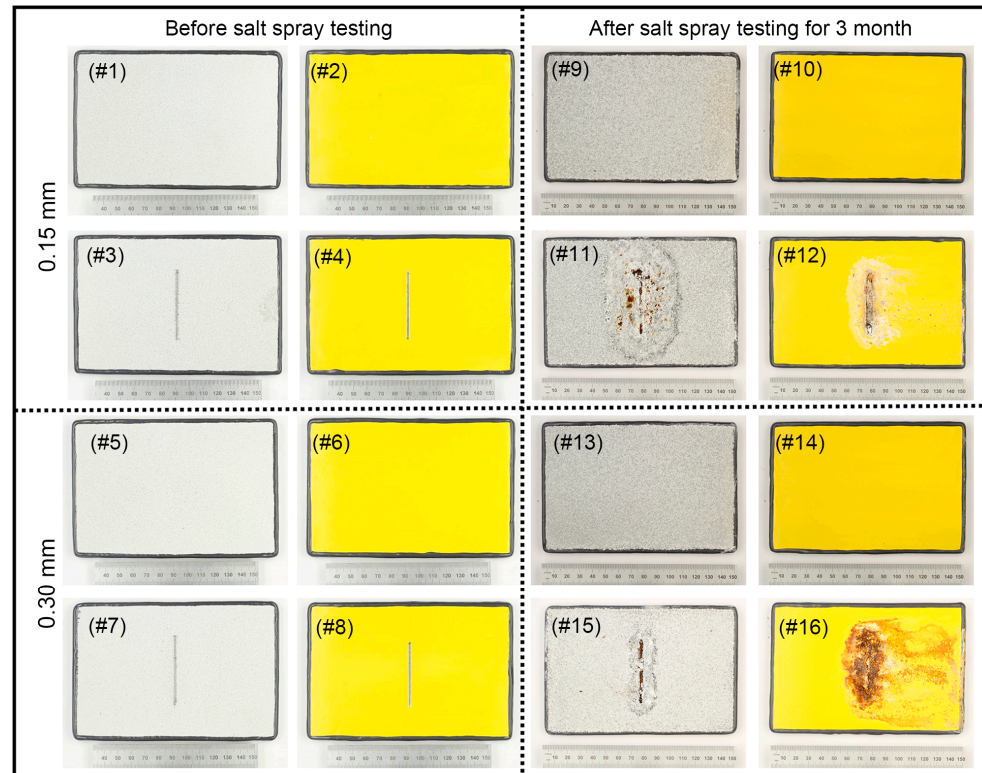


Figure 2. Macro morphology of Al coating samples before and three months after salt spray test. (#1) 0.15 mm coating sample before test, (#2) 0.15 mm paint sample before test, (#3) 0.15 mm coating sample with scribed lines before test, (#4) 0.15 mm paint sample with scribed lines before test, (#5) 0.30 mm coating sample before test, (#6) 0.30 mm paint sample before test, (#7) 0.30 mm coating sample with scribed lines before test, (#8) 0.30 mm paint sample with scribed lines before test, (#9) 0.15 mm coating sample after test, (#10) 0.15 mm paint sample after test, (#11) 0.15 mm coating sample with scribed lines after test, (#12) 0.15 mm paint sample with scribed lines after test, (#13) 0.30 mm coating sample after test, (#14) 0.30 mm paint sample after test, (#15) 0.30 mm coating sample with scribed lines after test, (#16) 0.30 mm paint sample with scribed lines after test.

3.1.2. Microstructure Observation

The SEM images and energy-dispersive spectroscopy (EDS) results of cross sections of Al-coated samples with scribed lines (#15) after salt spray test are illustrated in Figure 3. The coated sample disintegrated near the delineated area (Figure 3a). The EDS analysis of the scribed area showed the presence of corrosion products with Fe and O as the main components (Figure 3b). The Al coating far from the delineated area was also severely depleted by corrosion (Figure 3c). The BSE image revealed a clear contrast between the depleted Al coating and the intact Al, and the EDS data also demonstrated this (Figure 3d,f). The Al remained intact near the substrate; however, much of the Al was oxidized to Al-O or Al-O-H corrosion products in the area away from the substrate (Figure 3c,d). Although the Al coatings did not show significant pitting, some cracking was observed in the corrosion products formed because of the conversion of Al to Al-O and/or Al-O-H (Figure 3e).

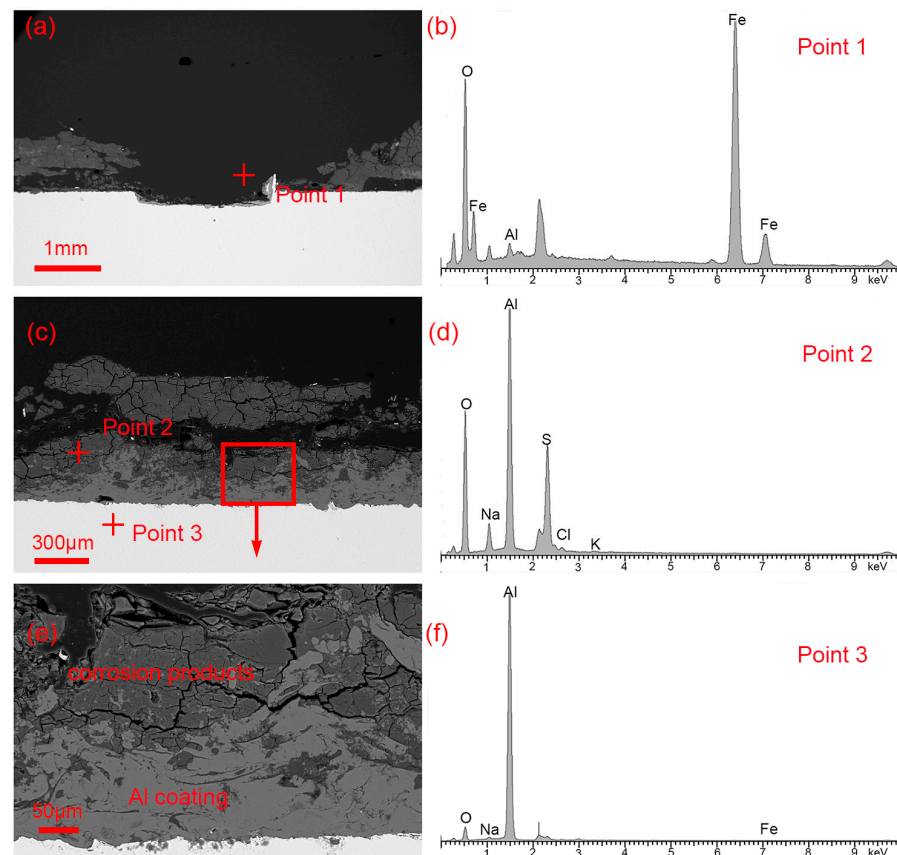


Figure 3. (a,c,e) SEM images of coating samples with scribed lines after 3 months of salt spray test. Some EDS patterns obtained from the region of interest are shown in (b,d,f).

Figure 4 provides the microstructure of the Al-coated sample with the paint layer (#16) after salt spray test. A large amount of corrosion products near the scribe line was observed (Figure 4a). These corrosion products included Fe and O as the main components near the steel substrate (Figure 4b), and Al and O away from the substrate (Figure 4d). The corrosion products appeared to be porous, with cracks in some areas. In the area away from the scribed line, the corrosion products appeared to propagate along the interface of the Al coating and paint layer. The corrosion products at the interface between Al and paint were Al–O and/or Al–O–H compounds (Figure 4e,f). The thickness of the Al corrosion products at the top of the Al coating decreased as it gradually moved away from the scribed area. In addition, some Al corrosion products can be seen inside the coating (Figure 4e).

As a result, despite three months of corrosion in a salt spray environment, the corrosion products mostly were mainly concentrated at the scribe lines and did not overly attack the substrate and other areas excessively. This demonstrates the excellent damage tolerance of the Al coating on the steel substrate, and is further enhanced by the use of a paint layer.

3.2. Immersion Test

3.2.1. Electrochemical Monitoring

Coated samples (#17 and #18) were subjected to OCP in 0.5 wt% NaCl and 3.5 wt% $(\text{NH}_4)_2\text{SO}_4$ for 3 months. Two samples were taken for each coating thickness to test reproducibility. The OCP of the bare steel substrate was also monitored for comparison. The relationship between open potential and time is shown in Figure 5. At the beginning, the exposed steel substrate showed an OCP of about 670 mv vs. Ag/AgCl, and then the OCP rapidly increased to about 740 mv vs. Ag/AgCl in a very short time. Then, OCP was basically stable at this level during the subsequent long period of foam invasion. The change trend of open potential of Al-coated samples is similar to that of steel. First, OCP is

at a small value (about 793 mv vs. Ag/AgCl). With the increase in time, OCP is suddenly increased. This may be because of the combined effect of some defects/pores and cracks on the coating surface, or it may be the anodic property of Al metal [24]. Therefore, the corrosive ions in the solution can easily penetrate and cause the rapid increase in OCP. When the time is 5 days, the OCP starts to decrease gradually until the end of the test. Finally, when the time is 94 days, the OCP is about 925 mv vs. Ag/AgCl.

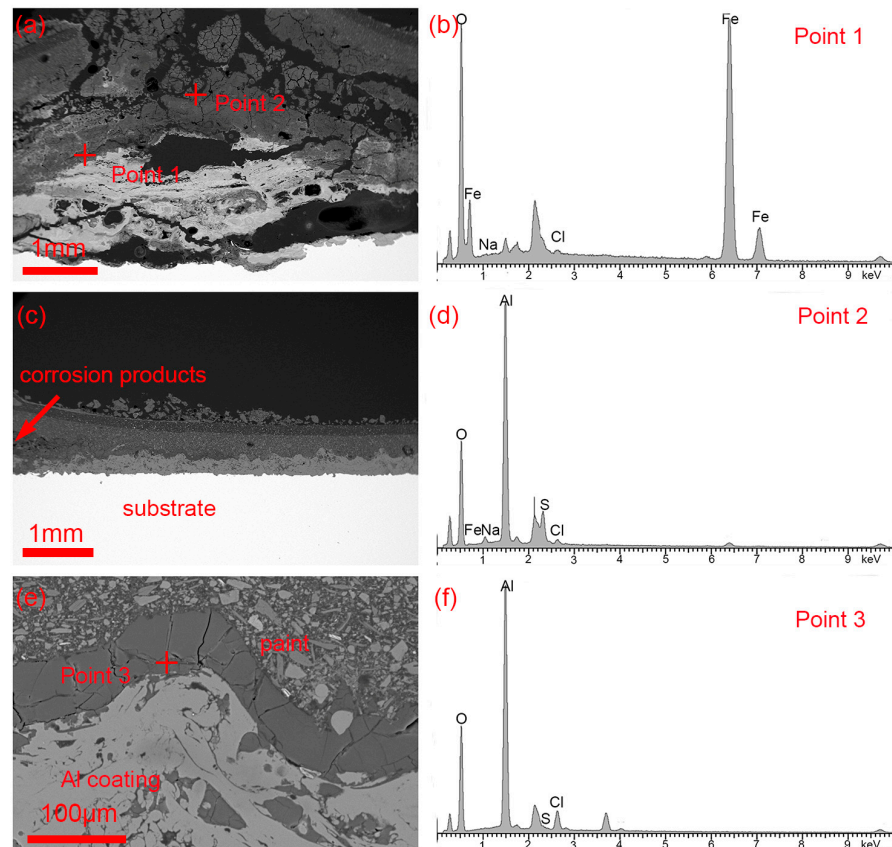


Figure 4. (a,c,e) SEM images of paint samples with scribed lines after 3 months of salt spray test. Some EDS patterns obtained from the region of interest are shown in (b,d,f).

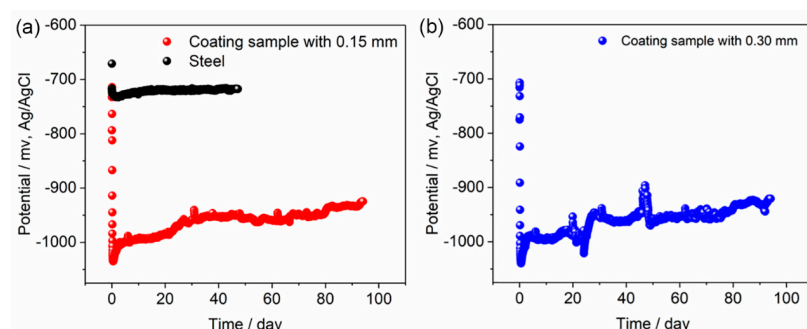


Figure 5. Open circuit potential of coatings tested in 0.5 wt% NaCl and 3.5 wt% $(\text{NH}_4)_2\text{SO}_4$ for 3 months. (a) 0.15 mm coating sample, (b) 0.30 mm coating sample. The data for base steel substrate are also shown for comparison.

From the point of view of open potential, it can be seen that the steel substrate was corroded in a very short time, and the coated samples affected the damage well. Moreover, the effect of coating thickness on OCP seemed to be minimal, and the OCP of samples with two coating thicknesses was always similar at the same time.

3.2.2. Corrosion Rate

The corrosion rates were calculated for two thicknesses of coating samples (#17 and #18) in 0.5 wt% NaCl and 3.5 wt% $(\text{NH}_4)_2\text{SO}_4$, as shown in Figure 6. The trend of corrosion rate was similar for both samples. The corrosion rate decreased rapidly within a short period of time. When the soaking time was about 5 days, the curve development entered the second stage, and the corrosion rate decreased significantly. A similar phenomenon has been widely reported. Campo et al. [25] suggested that the reason for this is that the early corrosion products will block the internal defects of the coating, thus inhibiting more penetration of the electrolyte into the coating, which in turn increases the impedance value of the coating and greatly reduces the corrosion rate. In the subsequent long-term test process, the corrosion rate almost does not change and reaches 0.002 mm/y to 0.005 mm/y after 3 months of testing.

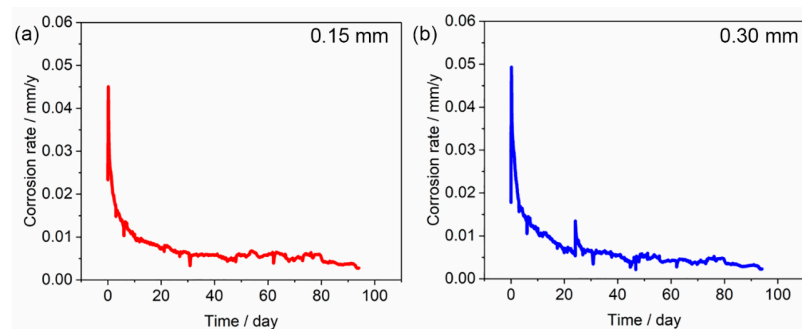


Figure 6. Corrosion rate of coatings tested in 0.5 wt% NaCl and 3.5 wt% $(\text{NH}_4)_2\text{SO}_4$ for 3 months. (a) 0.15 mm coating sample, (b) 0.30 mm coating sample.

Assuming a constant corrosion rate of 0.005 mm/y over the lifetime of the coating, it is theoretically possible to speculate that a coating with a thickness of 0.3 mm and no damage would last 60 years. However, it must be noted that this is a speculation based on the corrosion rate in a simulated environment. It is known that the corrosion rate varies with time, and thus the effective corrosion rate can at best be used as a guide [26].

3.2.3. Morphology after Test

Figure 7 shows the surface morphology of the coating (#17 and #18) with two thicknesses three months after the immersion test. During visual inspection, the coatings under immersion conditions showed signs of corrosion, and the coatings showed gray corrosion products. The corrosion products were clearly visible in some areas, and the sediments were emitted from the surface. In general, the amount of corrosion products in thin and thick Al coatings seemed to be similar. However, in the thin coating samples, it was observed that some corrosion products were more concentrated and the color was darker, which may be the locations where the corrosion was more serious.

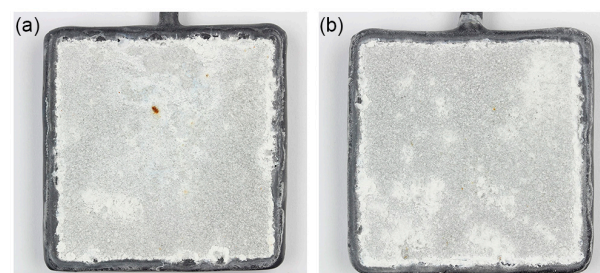


Figure 7. Photographs of (a) 0.15 mm and (b) 0.30 mm thick coating samples after the immersion test.

The microscopic morphology of the coating sample (#17) with a thickness of 0.15 mm after the immersion test is shown in Figure 8. The thin Al coating appeared to be largely

intact (Figure 8a), but some signs of corrosion products could still be observed on the coating surface (Figure 8b). The BSE images showed dark contrast, indicating no obvious corrosion products. The EDS results indicated that the main components of the corrosion products were Al and O (Figure 8c), and the presence of S in the corrosive medium was also evident in the EDS results. The coating appeared to have limited corrosion damage, except for a small amount of corrosion products at the coating surface. The EDS image also clearly showed that Al was still the dominant component (Figure 8d).

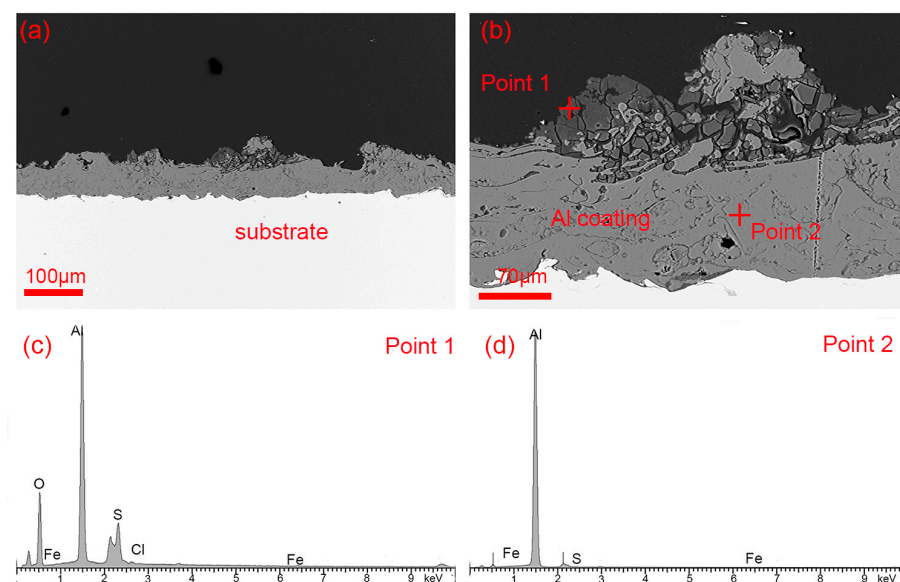


Figure 8. (a,b) SEM micrograph of the Al coating sample (~0.15 mm) after the immersion test for 3 months. EDS results of some areas in the figure are provided in (c,d).

Figure 9 shows the microscopic morphology of the coating samples (#18) with a thickness of 0.30 mm after three months of immersion. The thicker Al coating showed little evidence of corrosion damage (Figure 9a). Higher-magnification SEM images also indicated very limited coating damage (Figure 9b). The BSE images revealed that the coating was essentially intact, with only some corrosion products in some areas of the surface, and that these were sparsely distributed (Figure 9b). EDS maps of some areas of the surface suggested the presence of Al and O (Figure 9c). However, as mentioned earlier, the coating was essentially intact. The results of the XRD tests (Figure 10) also showed that the coating was not significantly corroded after 90 days of the immersion experiment and the sample remained essentially Al. Although the sample surface exhibited some corrosion products, it is possible that the corrosion products were too few to be detected here with other phases such as Al–O.

From the perspective of corrosion morphology, both coatings could protect the steel substrate well, but relatively speaking, thick coatings seemed to have better lasting effects.

3.3. Adhesion Test

Figure 11 shows the adhesion data of the Al-coated samples 0.30 mm before and after environmental test. The adhesion values of the samples before the tests ranged from 21 to 23 MPa, with an average value of about 22.16 MPa. This value was far greater than the adhesion (4.86 MPa) of 100 μm Al coating sprayed on the steel substrate by Singh et al. [27], and is also tested by the same test standard (ISO 2063) [28]. The distribution of these data indicates that the coatings were evenly distributed and had excellent adhesion. Although the average adhesion of the coatings decreased slightly after the salt spray test and the immersion test, 17.07 MPa and 19.25 MPa, respectively, it remained at a high level, well above the standard of 4.5 MPa (ISO 2063) [28]. In addition, the distribution of the five adhesion values of the post-corrosion coating samples was more dispersed than that of the

original coating samples because of the corrosion in certain areas, which was more evident in the samples of the immersion test. This may be because of the corrosion products on the surface preventing good adhesion of the adhesive/glue to the samples.

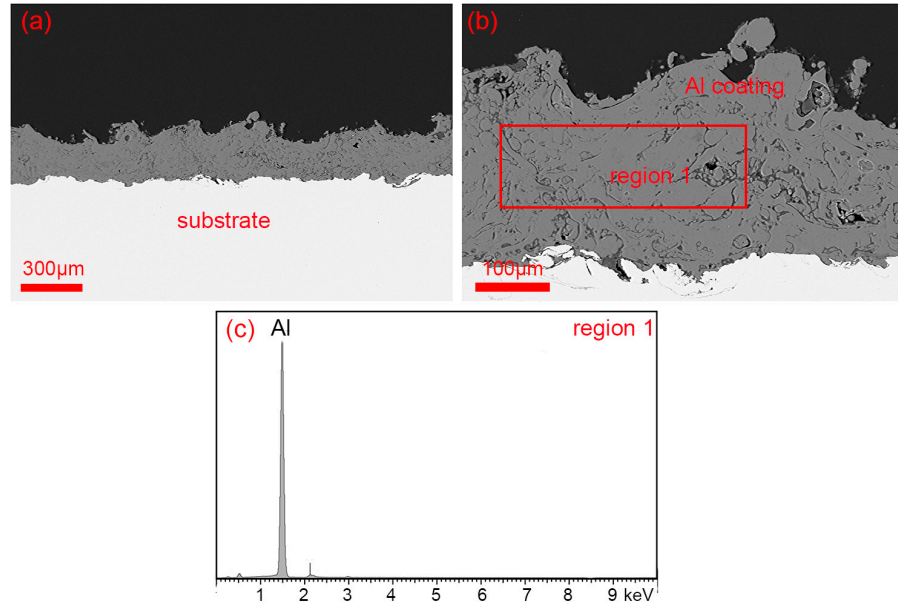


Figure 9. (a,b) SEM micrograph of the Al coating sample (~0.30 mm) after the immersion test for 3 months. EDS results of some areas in the figure are provided in (c).

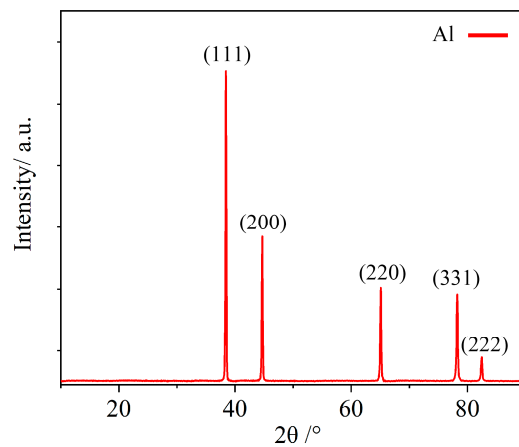


Figure 10. XRD results of the Al coating sample (~0.30 mm) after the immersion test for 3 months.

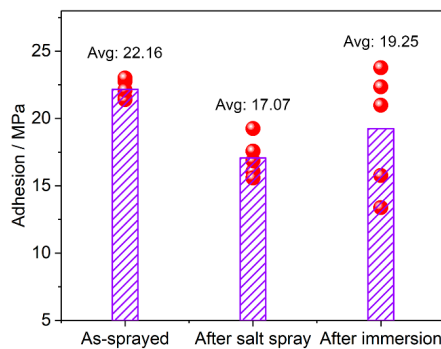


Figure 11. Adhesion of thermal spray coatings before and after testing.

By testing the microstructure evolution, corrosion resistance and adhesion of Al coatings under different conditions in a simulated acid rain environment, it was found that the Al coating samples with a thickness of 300 μm and sprayed with paint had better reliability. This provides theoretical guidance for the corrosion protection of transmission and substation equipment in highly corrosive environments. The Al alloy coating can be prepared by adding alloying elements in future research to explore whether the addition of alloying elements can further improve the reliability of the coating.

4. Conclusions

In this paper, the morphology, corrosion performance and adhesion of Al coatings under different conditions (different thickness, whether painted or damaged) after salt spray and immersion tests were studied. The main conclusions are as follows:

(1) The blasting parameters used to prepare the steel substrate were sufficient to produce a surface roughness in the required range of 50–100 μm . After thermal spraying, Al coating samples with complete morphology were obtained;

(2) The thicker Al coating showed better performance under the salt spray test conditions, and the painted samples more effectively protected the steel substrate. The damage test showed that only a small amount of corrosion products appeared at the scribed line, and the corrosion damage was limited;

(3) After immersion for 3 months, the corrosion rate of Al coating samples decreased to between 0.002 mm/y and 0.005 mm/y. Assuming that the constant corrosion rate during the whole life of the coating is 0.005 mm/y, it can be assumed theoretically that the coating with a thickness of 0.30 mm and no damage could be used for 60 years;

(4) After the salt spray test and immersion test, the average adhesion of the coating samples decreased slightly to 17.07 MPa and 19.25 MPa, respectively, but still far exceeded the required value;

(5) In summary, the protection effect of the coating on the steel substrate can be significantly enhanced by painting the surface of the thicker Al coating. The coating design of this structure broadens the idea of anti-corrosion Al coatings used for power transmission and transformation equipment, and can greatly improve the service life of the equipment.

Author Contributions: Conceptualization, B.L. and L.F.; methodology, Y.W., J.H. and J.S.; investigation, S.Z., S.L. and Z.Z. All authors have read and agreed to the published version of the manuscript.

Funding: This research was financially supported by the Science and technology project of China Southern Power Grid Co., Ltd. (Grant No. GZKJXM20191302).

Institutional Review Board Statement: Not applicable.

Informed Consent Statement: Not applicable.

Data Availability Statement: The data presented in this study are available on request from the corresponding author.

Conflicts of Interest: The authors declare no conflict of interest.

References

1. Zhang, X.; Chen, Z.M.; He, S.Z.; Hua, W.; Zhao, Y.; Li, J.L. Peroxyacetic acid in urban and rural atmosphere: Concentration, feedback on PAN-NO_x cycle and implication on radical chemistry. *Atmos. Chem. Phys.* **2010**, *10*, 737–748. [[CrossRef](#)]
2. Krom, M.D.; Shi, Z.; Anthony, S.; Ilana, B.F.; Antonia, G.; Barak, H.; Anna, L.; Nafsika, P.; Paraskevi, P.; Stella, P. Response of the Eastern Mediterranean Microbial Ecosystem to Dust and Dust Affected by Acid Processing in the Atmosphere. *Front. Mar. Sci.* **2016**, *3*, 133. [[CrossRef](#)]
3. Gao, Z.; Vasilakos, P.; Nah, T.; Takeuchi, M.; Chen, H.; Tanner, D.J.J.; Ng, N.L.; Kaiser, J.J.; Huey, L.G.G.; Weber, R.J.; et al. Emissions, chemistry or bidirectional surface transfer? Gas phase formic acid dynamics in the atmosphere. *Atmos. Environ.* **2022**, *274*, 118995. [[CrossRef](#)]
4. Jin, P. Mechanism of Corrosion by Naphthenic Acids and Organosulfur Compounds at High Temperatures. Ph.D. Thesis, Ohio University, Athens, OH, USA, 2013.

5. Wu, Y.; Duan, Y.; Qiu, J.; Gao, X.; Ma, H. A pH-responsive intelligent coating based on composite CaCO₃ microspheres for long-term corrosion protection of Q235 carbon steel. *Appl. Surf. Sci.* **2022**, *578*, 151980. [[CrossRef](#)]
6. Zheng, S.; Bellido-Aguilar, D.A.; Huang, Y.; Zeng, X.; Zhang, Q.; Chen, Z. Mechanically robust hydrophobic bio-based epoxy coatings for anti-corrosion application. *Surf. Coat. Technol.* **2019**, *363*, 43–50. [[CrossRef](#)]
7. Mert, B.D. Corrosion protection of aluminum by electrochemically synthesized composite organic coating. *Corros. Sci.* **2016**, *103*, 88–94. [[CrossRef](#)]
8. Lee, H.S.; Singh, J.K. Influence of calcium nitrate on morphology and corrosion characteristics of ammonium phosphate treated Aluminum coating deposited by arc thermal spraying process. *Corros. Sci.* **2019**, *146*, 254–268. [[CrossRef](#)]
9. Steenkiste, T.; Smith, J.R.; Teets, R.E. Aluminum coatings via kinetic spray with relatively large powder particles. *Surf. Coat. Technol.* **2002**, *154*, 237–252. [[CrossRef](#)]
10. Choi, W.B.; Li, L.; Luzin, V.; Neiser, R.; Gnäupel-Herold, T.; Prask, H.J.; Sampath, S.; Gouldstone, A. Integrated characterization of cold sprayed aluminum coatings. *Acta Mater.* **2007**, *55*, 857–866. [[CrossRef](#)]
11. Hall, A.C.; Brewer, L.N.; Roemer, T.J. Preparation of Aluminum Coatings Containing Homogenous Nanocrystalline Microstructures Using the Cold Spray Process. *J. Therm. Spray Technol.* **2008**, *17*, 352–359. [[CrossRef](#)]
12. Dietrich, D.; Wielage, B.; Lampke, T.; Grund, T.; Kümmel, S. Evolution of Microstructure of Cold-Spray Aluminum Coatings on Al₂O₃ Substrates. *Adv. Eng. Mater.* **2012**, *14*, 275–278. [[CrossRef](#)]
13. Bu, H.; Yandouzi, M.; Chen, L.; Jodoin, B. Effect of heat treatment on the intermetallic layer of cold sprayed aluminum coatings on magnesium alloy. *Surf. Coat. Technol.* **2011**, *205*, 4665–4671. [[CrossRef](#)]
14. Li, G.; Ma, Y.; Wan, H.; Chen, L.; An, Y.; Ye, Y.; Zhou, H.; Chen, J. Flake aluminum reinforced polyamideimide-polytetrafluoroethylene bonded solid lubricating composite coating for wear resistance and corrosion protection. *Eur. Polym. J.* **2021**, *152*, 110485. [[CrossRef](#)]
15. Feng, X.; Wang, H.; Liu, X.; Wang, C.; Cui, H.; Song, Q.; Huang, K.; Li, N.; Jiang, X. Effect of Al content on wear and corrosion resistance of Ni-based alloy coatings by laser cladding. *Surf. Coat. Technol.* **2021**, *412*, 126976. [[CrossRef](#)]
16. Li, P.; Huang, X.; Kong, D. Corrosive wear and electrochemical corrosion performances of arc sprayed Al coating in 3.5% NaCl solution. *Anti-Corros. Method Mater.* **2021**, *68*, 95–104. [[CrossRef](#)]
17. Ge, Y.; Cheng, J.; Wang, X.; Xue, L.; Liang, X.B. Formation and Properties of Superhydrophobic Al Coatings on Steel. *ACS Omega* **2021**, *6*, 18383–18394. [[CrossRef](#)] [[PubMed](#)]
18. Hui, Y.; Ji, H.; Chang, F.; Jian, G.; Guo, B. Microstructure and properties of TiC-Fe cermet coatings by reactive flame spraying using asphalt as carbonaceous precursor. *Ceram. Int.* **2007**, *33*, 827–835.
19. Mahu, G.; Munteanu, C.; Istrate, B.; Benchea, M.; Lupescu, S. Influence of Al₂O₃-13TiO₂ powder on a C45 steel using atmospheric plasma spray process. *IOP Conf. Ser. Mater. Sci. Eng.* **2018**, *444*, 032010. [[CrossRef](#)]
20. Sun, Z.; Zhang, D.; Yan, B.; Kong, D. Effects of laser remelting on microstructures and immersion corrosion performance of arc sprayed Al coating in 3.5% NaCl solution. *Opt. Laser Technol.* **2018**, *99*, 282–290. [[CrossRef](#)]
21. Ashraf, M.A.; Ahmed, N.; Khan, Z.S.; Iqbal, M.A.; Satti, A.N.; Farooq, A. Effects of Annealing Treatment on Corrosion Resistance of Arc Sprayed Aluminum Coating. *J. Therm. Spray Technol.* **2022**, *31*, 1934–1943. [[CrossRef](#)]
22. ASTM G59; Standard Test Method for Conducting Potentiodynamic Polarization Resistance Measurements. ASTM International: West Conshohocken, PA, USA, 2020.
23. ASTM D4541; Standard Test Method for Pull-Off Strength of Coatings Using Portable Adhesion Testers. ASTM International: West Conshohocken, PA, USA, 2022.
24. Tao, Y.; Xiong, T.; Sun, C.; Kong, L.; Kong, L.; Cui, X.; Li, T.; Song, G.L. Microstructure and corrosion performance of a cold sprayed aluminium coating on AZ91D magnesium alloy. *Corros. Sci.* **2010**, *52*, 3191–3197. [[CrossRef](#)]
25. Campo, M.; Carboneras, M.; López, M.D.; Torres, B.; Rams, J. Corrosion resistance of thermally sprayed Al and Al/SiC coatings on Mg. *Surf. Coat. Technol.* **2009**, *203*, 3224–3230. [[CrossRef](#)]
26. Balani, K.; Laha, T.; Agarwal, A.; Karthikeyan, J.; Munroe, N. Effect of Carrier Gases on Microstructural and Electrochemical Behavior of Cold-Sprayed 1100 Aluminum Coating. *Surf. Coat. Technol.* **2005**, *195*, 272–279. [[CrossRef](#)]
27. Singh, J.K.; Yang, H.; Lee, H.S.; Kumar, S.; Aslam, F.; Alyousef, R.; Alabduljabbar, H. Morphological and Corrosion Studies of Ammonium Phosphate and Caesium Nitrate Treated Al Coating Deposited by Arc Thermal Spray Process. *Surf. Interfaces* **2021**, *22*, 100885. [[CrossRef](#)]
28. ISO2063; Thermal Spraying—Zinc, Aluminium and Their Alloys—Part 2: Execution of Corrosion Protection Systems. International Organization for Standardization: Geneva, Switzerland, 2017.

Disclaimer/Publisher’s Note: The statements, opinions and data contained in all publications are solely those of the individual author(s) and contributor(s) and not of MDPI and/or the editor(s). MDPI and/or the editor(s) disclaim responsibility for any injury to people or property resulting from any ideas, methods, instructions or products referred to in the content.